Fabrication and Characterization of Drug-Loaded Conductive Poly(glycerol sebacate)/Nanoparticle-Based Composite Patch for Myocardial Infarction Applications

Ezazi, Nazanin Zanjanizadeh

2020-02-12

Ezazi , N Z , Ajdary , R , Correia , A , Mäkilä , E , Salonen , J , Kemell , M , Hirvonen , J , Rojas , O J , Ruskoaho , H J & Santos , H A 2020 , ' Fabrication and Characterization of Drug-Loaded Conductive Poly(glycerol sebacate)/Nanoparticle-Based Composite Patch for Myocardial Infarction Applications ' , ACS Applied Materials & Interfaces , vol. 12 , no. 6 , pp. 6899-6909 . https://doi.org/10.1021/acsami.9b21066

http://hdl.handle.net/10138/355561
https://doi.org/10.1021/acsami.9b21066

ACS APPLIED MATERIALS & INTERFACES

www.acsami.org

Research Article

Fabrication and Characterization of Drug-Loaded Conductive Poly(glycerol sebacate)/Nanoparticle-Based Composite Patch for Myocardial Infarction Applications

Nazanin Zanjanizadeh Ezazi, Rubina Ajdary, Alexandra Correia, Ermei Mäkilä, Jarno Salonen, Marianna Kemell, Jouni Hirvonen, Orlando J. Rojas, Heikki J. Ruskoaho, and Hélder A. Santos*

Cite This: *ACS Appl. Mater. Interfaces* 2020, 12, 6899–6909

Read Online

ACCESS | Metrics & More | Article Recommendations | Supporting Information

ABSTRACT: Heart tissue engineering is critical in the treatment of myocardial infarction, which may benefit from drug-releasing smart materials. In this study, we load a small molecule (3i-1000) in new biodegradable and conductive patches for application in infarcted myocardium. The composite patches consist of a biocompatible elastomer, poly(glycerol sebacate) (PGS), coupled with collagen type I, used to promote cell attachment. In addition, polypyrrole is incorporated because of its electrical conductivity and to induce cell signaling. Results from the in vitro experiments indicate a high density of cardiac myoblast cells attached on the patches, which stay viable for at least 1 month. The degradation of the patches does not show any cytotoxic effect, while 3i-1000 delivery induces cell proliferation. Conductive patches show high blood wettability and drug release, correlating with the rate of degradation of the PGS matrix. Together with the electrical conductivity and elongation characteristics, the developed biomaterial fits the mechanical, conductive, and biological demands required for cardiac treatment.

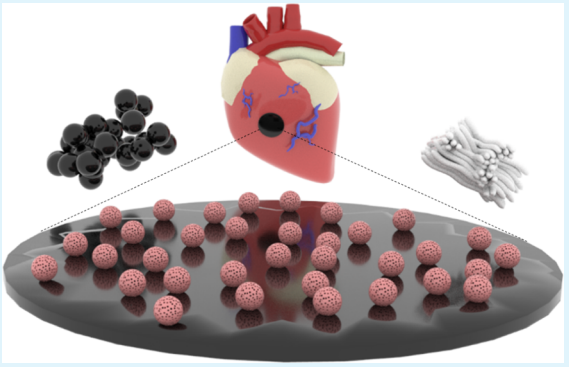

KEYWORDS: *heart tissue engineering, conductive polymers, polypyrrole, drug delivery, regeneration*

INTRODUCTION

Cardiovascular diseases (CVDs) include disorders of heart and blood vessels and are the most common cause for over 17 million deaths worldwide, as measured only in the year 2016.[1,2] Heart failure alone affects more than 23 million people globally and imposes a huge economic burden on societies. Heart failure is associated with increased morbidity and mortality and confers a substantial burden on the health-care system. Currently available treatments for heart failure include drug treatment, cardiac resynchronization therapy, mechanical support devices, and heart transplantation.[3] Although these techniques may apply for the majority of the patients and reduce the number of hospitalization instances, the long-term prognosis of patients with heart failure is poor. Due to the limitation of donor heart or applicability and efficiency of drugs in specific tissues, along with their adverse effects and thrombosis in the implant sites,[3,4] novel and advanced techniques are now at the center of attention to reduce the burden of morbidity and mortality associated with heart failure. In this regard, tissue engineering emerges as a promising approach to advance cardiovascular medicine. By adopting different materials and formulations, biomaterials can fulfill clinical needs, such as regeneration or repair of the damaged tissue toward improved structures and functions.[5] In fact, heart tissue engineering (HTE) has been shown to promote the recovery of the infarcted heart muscle after blockage of the coronary arteries.[6]

Biodegradable composite patches pioneer tissue engineering therapy. Such composites can be tailored to the physicochemical demands for heart therapy and tissue regeneration, including surface chemistry, electrical conductivity, and degradation profile.[7] The composites can be applied to the infarcted area of the heart and help the recovery, while gradually degrading over time without any need for a secondary surgery for removal.[8,9] The biocomposites can be loaded with drugs for delivery before complete patch degradation.[10] In such uses, the given engineered biomaterials[11] can be considered as carriers, including nanoparticles,[12,13] films,[14] microneedle systems,[15] and fibers.[16]

We use poly(glycerol sebacate) (PGS), an elastic polyester, for the 2D heart patches. PGS is easily synthesized by the polycondensation of nontoxic sebacic acid and glycerol, both

Received: November 19, 2019
Accepted: January 22, 2020
Published: January 22, 2020

approved by the U.S. Food and Drug Administration (FDA) as pharmaceutical products.[17] Soft, hydrated elastic PGS is suitable for cell culturing[17−19] and mechanically suitable for the dynamic demands[20] of the heart tissue. The physical properties of PGS can be tailored by curing temperature and time[20,21] and can be coupled by different polymers to make a composite with customized properties[22,23] and drug delivery profiles.[24] For example, PGS has been electrospun with gelatin to make aligned nanofibrous webs for HTE, inducing synchronous contractions of cardiomyocytes.[22] Collagen, the most abundant protein in the human body[25] and myocardium extracellular component,[26] has been also used with PGS to induce cell attachment and proliferation, for example, as an electrospun system for myocardial infarction applications.[25] PGS/collagen core/shell fibers developed by Ravichandran et al. showed a high attachment of cardiomyocytes−mesenchymal stem cells on the scaffold.[25] In addition, PGS can incorporate a conductive polymer to endow electrical conductivity.[27] For example, polypyrrole (PPy) has been used for diverse applications[28] owing to its excellent cell biocompatibility[5,29] and conductivity.[29] However, due to its poor mechanical strength and brittleness, PPy usually is combined with other polymers.[30,31]

Despite the few reports on conductive PGS composites for HTE, coupling with drug delivery systems has remained challenging. Here, we engineer smart thin films comprising PGS used as a (elastic hydrophilic) matrix together with collagen (for cell attachment) and PPy (for electrical conductivity), which form a composite ideal for the myocardial infarction application. The physicochemical properties and in vitro evaluation, cardiomyoblast viability, and attachments are studied. (3-Aminopropyl)triethoxysilane-functionalized thermally carbonized porous silicon nanoparticles (APTES-TCPSi NPs)[32] are attached on the surface of the conductive composite patch to investigate the functionalization ability of the surface. In addition, the proposed system is loaded with a model drug 3i-1000 to examine its delivery potential. The compound 3i-1000 is a small molecule inhibitor of GATA4-NKX2-5 transcriptional synergy, inhibiting a cardiomyocyte hypertrophic response and promoting the myocardial repair and regeneration in experimental models of myocardial infarction and hypertension.[33−36] We present a smart drug-loaded conductive biodegradable patch with a surface that can be functionalized by NPs for cardiac applications. Its easy processing and shape customizability make the proposed smart system suitable for implantation on the surface of the infarcted heart muscle, offering a new option for the treatment of related conditions.

MATERIALS AND METHODS

Materials. PPy, sebacic acid, and glutaraldehyde solution (25 wt % in H_2O) were purchased from Sigma-Aldrich. Glycerol 85% was purchased from Yliopiston Apteekki, Finland. Sodium dodecyl sulfate (SDS), dimethylsulfoxide (DMSO), and 4-(2-hydroxyethyl)-1-piperazineethanesulfonic acid (HEPES) were purchased from Sigma-Aldrich. Phosphate-buffered saline (PBS) 10×, FBS, Dulbecco's modified Eagle medium (DMEM), L-glutamine, nonessential amino acids (NEAAs), and penicillin−streptomycin were purchased from HyClone. Hank's buffered salt solution (HBSS) 10× was obtained from Gibco Life Technologies, and micro-bicinchoninic acid (BCA) protein assay kit was obtained from Thermo Fisher Scientific. The small molecule compound 3i-1000 was purchased from Pharmatory Ltd. (Oulu, Finland). 1,1,1,3,3,3-Hexafluoro-2-propanol (HFIP) was purchased from abcr, Germany, and Collagen Type I, Calf Skin Lyophilized was obtained from EPC.

Preparation of the Conductive Composite Scaffold. Composite cardiac patches were prepared from PGS, collagen, and PPy by the evaporation method. First, pre-PGS was synthesized by the polycondensation of an equimolar mixture of glycerol and sebacic acid.[37] Sebacic acid was weighted and moved to a clean two-neck flask that was later closed by a plastic cap and a two-layer balloon filled with argon gas. The remaining air inside the container was sucked out by a vacuum system and replaced with argon gas. Then, glycerol was added dropwise through a plastic cap by a syringe equipped with a long flexible needle. The mixture was moved to the paraffin oil bath at 120 °C for 24 h on a low-speed stirring. The formed pre-PGS was dissolved in HFIP before the prepolymer viscosity was raised, followed by the addition of 0.5% w/v (in HFIP) collagen. PPy solutions (1 and 5% w/v [in water]) were tip-sonicated by a high-intensity ultrasonic processor in a 40% amplitude before adding to the pre-PGS/collagen to make a dark black color mixture.[5] The suspension was mixed (600 rpm, 48 h) until it reached homogeneity. The suspension was poured into a round, self-made, silicone (Zhermack ZA22) mold (details in the Supporting Information (SI)). The HFIP was then evaporated overnight and later cured at 120 °C under a high vacuum for 48 h to obtain the elastic conductive heart patch. In total, different types of patches were made using different percentages of PPy and collagen: 0% collagen−0% PPy (0C−0P); 0% collagen−1% PPy (0C−1P); 0.5% collagen−0% PPy (0.5C−0P); 0.5% collagen−1% PPy (0.5C−1P); and 0.5% collagen−5% PPy (0.5C−5P).

Functionalization of the Conductive Elastic Cardiac Patch with PSi NPs. To check the activity of the surface of the patch, hydrophilic (3-aminopropyl)triethoxysilane-functionalized thermally carbonized porous silicon nanoparticles (APTES-TCPSi)[32] were chosen to be functionalized on the surface of the 0.5C−5P patch. Before adding the particles on the surface of the patch, 1 mL of *N*-hydroxysuccinimide (NHS)/(1-ethyl-3-(3-dimethylaminopropyl)-carbodiimide hydrochloride) (EDC) (10 μM) in 2-(*N*-morpholino)-ethanesulfonic acid MES (pH 5.5) mixture was added into each replicate at 4 °C in an icebox. Afterward, 1 mg of APTES-TCPSi NP was added to each solution on a shaker at 600 rpm for 12 h. The samples were washed with water and ethanol 10 times and were dried at 37 °C. Another set of samples were immersed in MES without cross-linkers and added to 1 mg of the APTES-TCPSi NP solution on a shaker at 600 rpm for 12 h, followed by washing 10 times with ethanol and water and drying at 37 °C.

Physiochemical Properties. The chemical structure of the samples was investigated by Fourier transform infrared (FTIR) spectroscopy, using a Vertex 70 spectrometer (Bruker Optics GmbH) equipped with a MIRacle horizontal attenuated total reflectance accessory (Pike Technologies Inc.) resolution of 4 cm^{-1}.

Thermogravimetry (TG) analysis of the samples was performed with a TGA-7 (PerkinElmer Inc.) system under a N_2 flush of 200 mL min^{-1} using a heating ramp of 20 °C min^{-1}. Differential scanning calorimetry (DSC) measurements were done with the Pyris Diamond DSC (PerkinElmer Inc.) using a heating ramp of 10 °C min^{-1} with a N_2 flush of 40 mL min^{-1}. A CAM 200 optical contact angle meter from KSV Instruments Ltd. equipped with a CCD camera module was used to image and calculate the wetting angle between the blood drops on the surface after 2 s. The wetting angle was obtained by calculating the average amount of two contact angles from both sides, using Attension Theta software.

Conductivity. A Jandel Model RM3000 four-point probe test unit combined constant current source and digital voltmeter was used to measure the sheet resistance of cardiac patches. The conductivity, C (S cm^{-1}), was calculated using the formula $C = [1/(R \times t)]$,[31] where R is measured in units of Ohms $square^{-1}$, and t is the film thickness in centimeters. A caliper was used to measure the thickness of each sample, and the reported values are the average of five replications.

Mechanical Properties. The composite patches were made following the same process as explained before by adding collagen (0.5%) and PPy (5%) to pre-PGS at 120 °C for 24 h under low

https://dx.doi.org/10.1021/acsami.9b21066
ACS Appl. Mater. Interfaces 2020, 12, 6899−6909

rotating speed. The suspension was cast in the form of a dog bone shape using a silicon (Zhermack ZA22) mold following the ASTM D638 standard (details in the SI). The HFIP evaporated overnight, and the prepolymer was cured at 120 °C under a high vacuum, using a vacuum oven for 48 h. Half of the samples were detached from the mold and immersed in 3 mL of 1× PBS (pH 7.4) for 21 days. The samples were dried at 37 °C for 24 h. The tensile properties were tested with a Universal Instron 4240 testing machine using a 100 N load. The test speed was 3 mm min^{-1}, and the gauge length was 30 mm. The tensile test samples were kept at room temperature and in a 50% controlled humidity room for 24 h before performing the test. The elastic modulus was calculated directly using software.

Degradation and Swelling. The samples were cut by a round cutter in same sizes and weighted (W_0) before immersing in 3 mL of 1× PBS (pH 7.4) at 37 °C to analyze the degradation percentage during 21 days (replicates of three). At each time point, the samples were vacuum-dried at room temperature for 24 h and weighed again to obtain (W_D). The degradation was calculated as: degradation % = $(W_0 - W_D) \times 100/W_0$.

In addition, to study the degradation speed in different media, the degradation study was done in ethanol and 0.1 M of NaOH, and compared with 1× PBS (pH 7.4) at 24 h. At the same time, the swelling behavior was also studied in the same media. A round cutter was used to cut the samples with the same size. They were weighed (W_0) and immersed into 3 mL media. After 24 h, the samples were wiped with a filter paper to absorb the medium on the surface and weighted in a wet state (W_S), and the swelling was calculated as Swelling % = $(W_s - W_0) \times 100/W_0$.

Protein Adsorption. The BCA protein assay was used to investigate the protein adsorption (first phenomena after scaffold implantation) on the patch surfaces. Conductive and nonconductive samples were kept at the bottom of the 48-well plates, using a Pyrex cylinder, where they were washed with ethanol and 1× PBS (pH 7.4). Afterward, a 1× PBS + 10% FBS solution was added to the samples and incubated for 4, 14, and 24 h at 37 °C to study the role of time in the adsorption of the proteins on the surface of the cardiac patch. Loosely attached proteins were washed away in two steps. First, a filter paper was used to gently remove the liquid on the surface, and then the samples were moved to a new 48-well plate and washed by 1× PBS several times. The adsorbed protein was recovered by 2% sodium dodecyl sulfate (SDS) and analyzed by a micro-BCA protein assay kit (Thermo Scientific Inc.), based on the manufacturer's protocol and measured by a Varioskan Flash plate reader (Thermo Scientific Inc. Fisher).

Drug Release Tests. 0.5C−5P samples were prepared by adding sonicated 5% PPy and 0.5% collagen suspensions in tetrahydrofuran (THF)/HFIP to pre-PGS. A volume of 0.5 mL of the suspension was pipetted out into the glass bottles, and 2 mg in 0.5 mL of 3i-1000 inside the THF was added. THF was evaporated overnight, and the drug-loaded patches were sintered at 120 °C for 48 h in a vacuum oven. Three samples were sintered without loading the compound and used as controls. The 3i-1000-loaded patches were immersed in the MES solution (5 mL, pH 6) and 1× PBS (5 mL, pH 7.4), corresponding to the conditions prevalent in infarcted heart[38] and physiological environments; they were further incubated at 37 °C for 80 days to check the role of pH in drug release. In addition, functionalized APTES-TCPSi NPs on 0.5C−5P and blank 0.5C−5P surfaces were immersed in the 2 mg mL^{-1} of 3i-1000 solution for 2 h and washed one time with water and immediately immersed in MES (pH 6) and 1× PBS (pH 7.4) to study the release of the adsorbed and NP-loaded 3i-1000 on the surface of 0.5C−5P. At each time point, 1 mL of the medium was replaced by an equal volume of a fresh medium. The release study was analyzed by high-performance liquid chromatography (HPLC) (Agilent 1260, Agilent Technologies). The HPLC conditions were: column Gemini NX-C18 (100 × 4.6 mm^2, 3 μm, Phenomenex, Denmark), a flow rate of 0.9 mL min^{-1}, and an injection volume of 20 μL with a mobile phase of 0.1% phosphoric acid (PA)/methanol (65:35 v/v) were used to study the release of the model drug. The column temperature was kept at 25 °C, and the detection wavelength used was 280 nm. The released amount of compound in each time point was calculated by integrating the total area under the peaks of the detected 3i-1000 in each sample.

Cell Viability. The samples were sterilized under a UV lamp for 3 h and transferred to 48-well plates, where they were kept at the bottom of each well using Pyrex cylinders (Thermo Fisher Scientific Inc.). To each well of the samples and the empty well + Pyrex cylinders were added by fresh DMEM + 10% FBS and 1% (w/v) L-glutamine, 1% (w/v) NEAA, and penicillin−streptomycin (100 IU mL^{-1}) and stored for 24 h at 37 °C in 5% CO_2. About 10 000 cardiomyoblast rat cells (H9c2(2-1) (ATCC CRL1446), USA) were seeded on top of each patch and kept at 37 °C in 5% CO_2. The old medium was discarded every 2 days and was replaced by fresh DMEM + 10% FBS and antibiotics. At each time point, AlamarBlue cell viability reagent (Thermo Fisher Scientific) was used to analyze the cell proliferation.

DMEM + 10% AlamarBlue was added to each well of the samples, where the positive control were the empty well + Pyrex cylinders and the negative control was 1% Triton X-100, and stored in an incubator for 6 h in the dark before measuring. The fluorescent resorufin solution was collected and moved into opaque 96-well plates, and the proliferation was measured by a Varioskan Flash plate reader (Thermo Fisher Scientific Inc.). In addition, prepolymer composited was cast in four replicates of glass bottles, and to it was added 2 mg 0.5 mL^{-1} of 3i-1000 inside THF. Glass bottles were used to cast the prepolymer without the compound 3i-1000 and used as control. After the solvent evaporation and curing step in a vacuum oven, the samples were sterilized under UV for 3 h and immersed in DMEM + 10% FBS for 24 h in the incubator at 37 °C in 5% CO_2. About 10 000 H9C2 cells were seeded into all of the glass bottles covered by a flask cap with a filter. At each time point, the viability of the cells was evaluated by the AlamarBlue assay.

In addition, the 3-(4,5-dimethylthiazol-2-yl)-2,5-diphenyltetrazolium bromide (MTT) assay was utilized to examine the cytotoxicity of patch degradation by the extract method for 21 days. Five replicates of each UV-sterilized sample were immersed inside DMEM + 10% FBS and 1% (w/v) L-glutamine, 1% (w/v) NEAA, and penicillin−streptomycin (100 IU mL^{-1}) at 37 °C in 5% CO_2 in 48-well plates for 28 days. At the same time, a blank control of DMEM + 10% FBS was incubated in the same condition for 21 days. Separately, 24 h before each time point of days 1, 7, 14, 21, and 28, about 10 000 myoblast H9C2 cells were seeded inside a fresh medium in a 96-well plate for each type of sample, including the positive (incubated medium) and negative (1% Triton X-100) controls. At each time point, the medium of each well in the 96-well plates was replaced by the medium of the incubated samples, as well as the positive (blank medium) and negative (1% Triton X-100) controls. The well plate was incubated for 24 h at 37 °C in 5% CO_2. Next, each well was washed twice with PBS buffer (pH 7.4), and 100 μL of the MTT solution (0.5 mg mL^{-1}) in HBSS−HEPES (pH 7.4) was added and incubated in the dark for 4 h. To each sample was added 100 μL of DMSO and kept on a shaker for 10 min. The formazan was collected from each well into a new transparent 96-well plate and was measured by a Varioskan Flash plate reader (Thermo Scientific Inc.).

Cell Attachment. Cardiomyoblast morphology and attachment were investigated on the surface of cardiac patches using a scanning electron microscope (SEM), Hitachi S-4800. Samples were sterilized under UV for 3 h and kept in DMEM + 10% FBS and 1% (w/v) L-glutamine, 1% (w/v) NEAA, and penicillin−streptomycin (100 IU mL^{-1}) at 37 °C in 5% CO_2 in 48-well plates for 24 h. Near 20 000 myoblast H9C2 were seeded on the samples that were kept at the bottom of the well using Pyrex cylinders. After 24 h, the samples were washed twice with PBS buffer (pH 7.4) and fixed by 2.5% glutaraldehyde in 1× PBS at 37 °C for 1 h, followed by postfixation, using 1% osmium tetroxide in PBS for 1 h. Afterward, the cells were dehydrated using different concentrations of ethanol (50, 70, 96, and 100%). The samples were coated with 5 nm of gold−palladium alloy prior to imaging and evaluated using an acceleration voltage of 10 kV.

Statistical Analysis. The results are expressed as mean ± standard deviations (SD) of at least three independent sets of measurements. Statistical analysis was done using a one-way analysis

https://dx.doi.org/10.1021/acsami.9b21066
ACS Appl. Mater. Interfaces 2020, 12, 6899−6909

Scheme 1. Schematic Illustration of the Steps Used for the Synthesis of Conductive and Elastic Biodegradable Cardiac Patches Using the Evaporation Method[a]

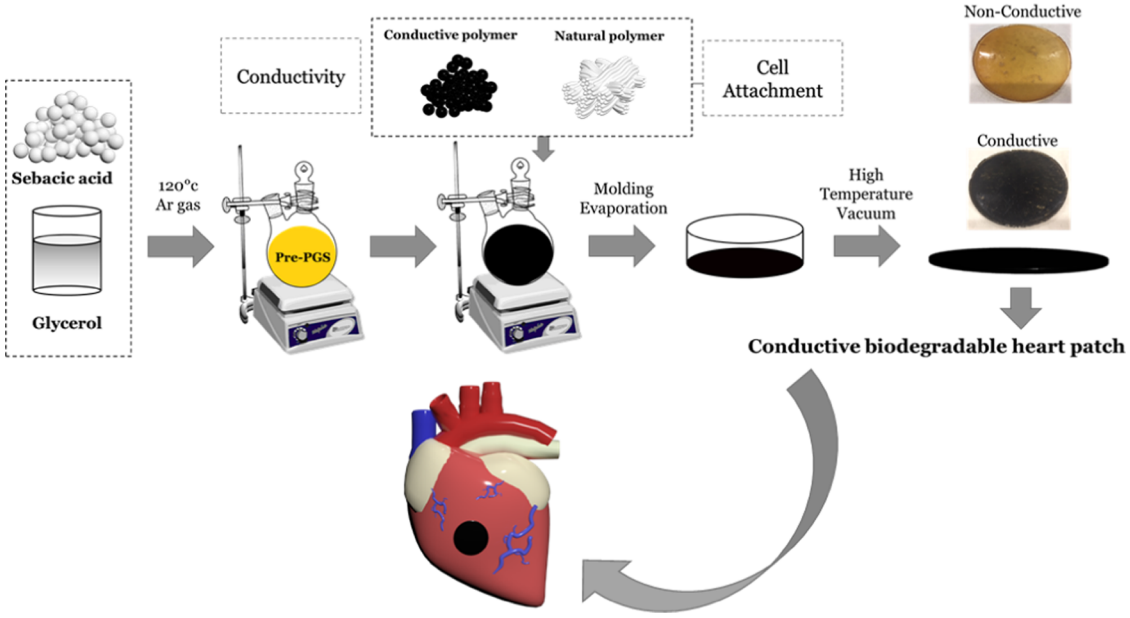

[a]Polycondensation of sebacic acid and glycerol was used to prepare pre-PGS, followed by the addition of collagen type I and conductive PPy. The solvent was evaporated, and the precomposite polymer was cured at high temperature under vacuum.

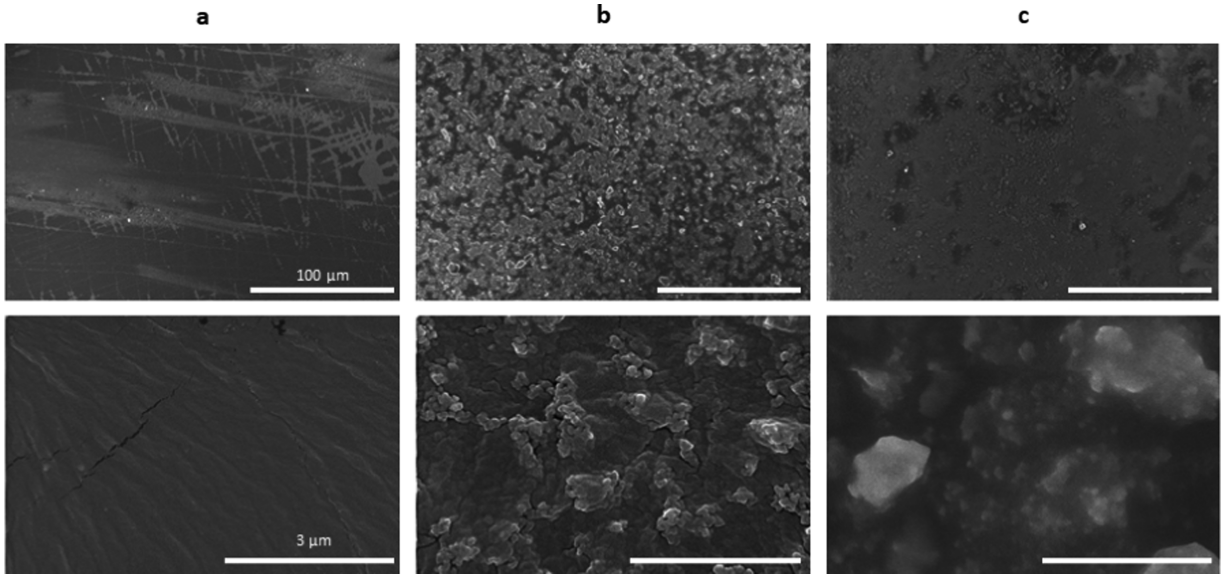

Figure 1. Surface morphology (SEM) of (a) blank 0.5C−5P, (b) 0.5C−5P functionalized with APTES-TCPSi NPs, and (c) 0.5C−5P carrying adsorbed APTES-TCPSi NPs, without cross-linking. The scale bars correspond to 100 μm (top) and 3 μm (bottom).

of variance (ANOVA) with the level of significance set at probabilities of $*p < 0.05$, $**p < 0.01$, $***p < 0.001$, analyzed with OriginPro8.6 software (OriginLab Corp.).

RESULTS AND DISCUSSION

To evaluate the capability of degradable heart patch to release the model drug for HTE application, we propose the conductive and elastic PGS-based patches loaded with 3i-1000 using the simple casting and evaporation method. We first started by synthesizing the conductive patch, as shown in Scheme 1, where the processing steps are illustrated. Pure PGS of 0% collagen−0% PPy (0C−0P), 0% collagen−1% PPy (0C−1P), and 0.5% collagen−0% PPy (0.5C−0P) samples were used as control and for comparison with 0.5% collagen−5% PPy (0.5C−5P) patches.

Table 1. Conductivity of Various Ratios of the 2D Cardiac Patch

sample	C (S cm^{-1})
0C−0P	0
0.5C−0P	0
0C−1P	partial conductivity 0.009−0.011
0.5C−1P	0
0.5C−5P	0.06 ± 0.14

https://dx.doi.org/10.1021/acsami.9b21066
ACS Appl. Mater. Interfaces 2020, 12, 6899−6909

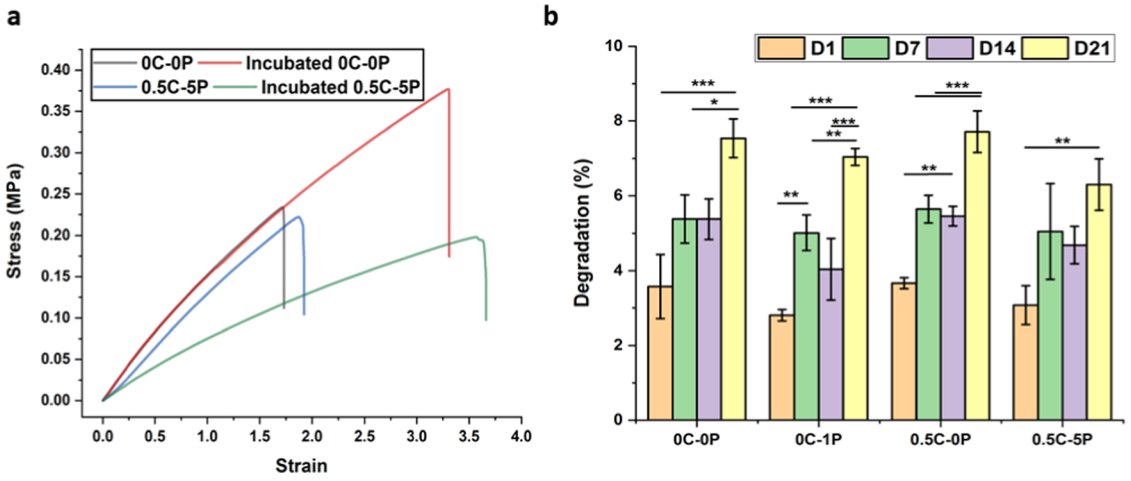

Figure 2. (a) Mechanical stress−strain curve of dry and incubated 0C−0P and 0.5C−5P composites in 1× PBS (pH 7.4) for 21 days. (b) Degradation percentage of 0C−0P, 0C−1P, 0.5C−0P, and conductive 0.5−5P during 21 days. Statistical analysis was achieved by means of a one-way analysis of variance (ANOVA), with the level of significance set at probabilities of $^{**}p < 0.01$ and $^{***}p < 0.001$.

Table 2. Mechanical Properties of the Samples Before and After PBS

sample	modulus (MPa)
0C−0P	0.17
incubated 0C−0P	0.17 ± 0.01
0.5C−5P	0.14 ± 0.04
incubated 0.5C−5P	0.08

Surface Morphology. The functionality of the conductive patch was examined by attaching the NPs on the surface. The surface morphology of blank, functionalized 0.5C−5P and absorbed APTES-TCPSi NPs[32] on 0.5C−5P was analyzed by SEM, using Hitachi S-4800. PGS, collagen, and PPy composite formed a uniform and homogeneous structure (Figure 1a), which is suitable for cell attachment and functionalization. APTES-TCPSi NPs were functionalized and adsorbed on 0.5C−5P and formed a rough surface, as shown in Figure 1b,c, respectively. The functionalized and adsorbed NPs on the surface of the composite were confirmed by energy-dispersive X-ray spectroscopy (EDX) (Figure S1a). The physical adsorption without cross-linkers could not show an efficient NP attachment, and the NPs were easily detached during the washing steps by water and ethanol (Figure 1c). Due to the hydroxyl and carbonyl groups on the surface of the patch (Figure S1b), NPs can be functionalized using NHS and EDC chemistry to facilitate coupling via amidation.[39] NPs coupled on the surface retained their morphology (Figure 1b) and remained stable after washing. FTIR spectra show the hydroxyl (−OH) stretching bond around 3500 cm^{-1} and the ester bonds of (C═O) at 1730 cm^{-1}, which is due to the carbonyl stretching vibration. The stretching ($-CH_2$) is shown at 2850, and 2925 and 1169 cm^{-1}, representing the C−O−C stretching peak. The amides I and II of collagen (around 1638 and 1554 cm^{-1})[25,31,40,41] and PPy bands of the bending and stretching of amine groups (1560 and 880 cm^{-1})[31] are properly masked. These active groups on the surface of the PGS matrix suggest the high potential of the surface for functionalization with the amine-terminated PSi NPs.

Physicochemical Characterization. TG and DSC were used to compare the thermal properties of the composite and pure PGS. Both methods show that the thermal properties of the composite patch of 0.5C−5P are similar to those of the pure PGS (Figure S1c). Both 0.5C−5P composite and pure PGS (0C−0P) degrade nearly completely, with the degradation starting at ca. 465 °C, leaving behind ca. 1−2 wt % of residue. The DSC results show that there are no phase transitions occurring below 200 °C, with the broad endotherm below 110 °C appearing as drying of the sample. In general, the addition of collagen and PPy to the PGS matrix did not appear to change the thermal properties of PGS.

In addition, the crystallinity and TGA/DSC analysis of pure 3i-1000 (Figure S4a,b) were done to check the stability of the compound. The XRD confirmed the initial crystallinity of the pure drug, with the DSC results showing only one endothermic peak after 120 °C, corresponding to the melting of 3i-1000 crystals. Moreover, the wettability was studied by both qualitative and quantitative methods (Figure S2). After the implantation of the biomaterials inside the body, proteins and blood will cover the surgery area.[42] As a result, the blood wettability test was done to study the wetting behavior of patches inside the human blood (obtained from anonymous donors from the Finnish Red Cross). Conductive and pure PGS patches (around 10 mm in diameter) were immersed in 3 mL of blood in sterile conditions and pictured after 5 s and 48 h. First, 0C−0P and conductive patches of 0.5C−5P were sterilized and immersed in 1 mL of blood for 5 s, and the wetting ability was observed. The same samples were immersed in blood for 48 h inside the incubator at 37 °C in 5% CO_2. The samples were washed twice with water and again immersed in blood samples, and the wettability was observed again.

The results showed that the conductive composite containing 5% of PPy has higher blood wettability compared with the pure PGS at two different time points. However, the quantitative results show the same range of contact angle of $\theta = 59.35° \pm 12.2$ for 0C−0P and $\theta = 55.51° \pm 4.9$ for 0.5C−5P, which is due to the O−H group[40] on the pure PGS, showing its hydrophilic properties. The qualitative image results are due to the PPy, the hydrophobic characteristics of which[41] make the composite more hydrophobic compared with the pure PGS. It has been reported that the hydrophobic surfaces are able to adsorb protein C3, fibronectin, and vitronectin to a greater extent compared with the hydrophilic surfaces. In addition, platelets and leukocytes in blood have higher

https://dx.doi.org/10.1021/acsami.9b21066
ACS Appl. Mater. Interfaces 2020, 12, 6899−6909

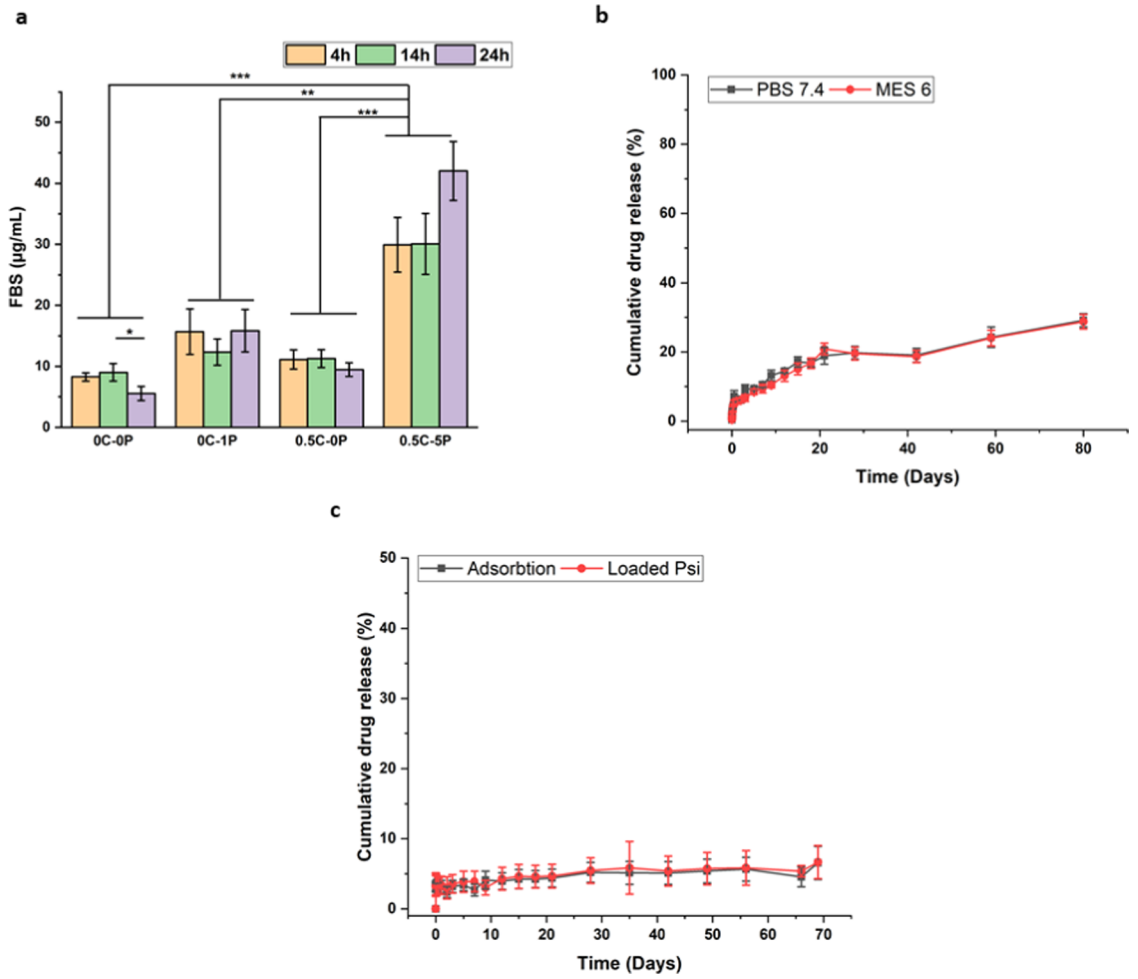

Figure 3. (a) Protein adsorption on 0C−0P, 0C−1P, 0.5C−0P, and 0.5C−5P patch surfaces at three different time points of incubation of the conductive and control patches. (b) Cumulative 3i-1000 release percentage from the bulk of degradable conductive patch of 0.5C−5P in 1× PBS (pH 7.4) and MES (pH 6). (c) Cumulative release in the MES buffer (pH 6) of 3i-1000 drug initially adsorbed on the surface and loaded in functionalized APTES-TCPSi NPs. Statistical analysis was obtained using a one-way analysis of variance (ANOVA), with the level of significance fixed at probabilities of $^{**}p < 0.01$ and $^{***}p < 0.001$.

absorbance in the hydrophobic samples.[42,43] Platelets are attached to the hydrophobic surfaces after 5 s,[42,43] which can help to wet the PPy-based composite more than PGS.

Conductivity. In tissue engineering applications, adequate electrical conductivity is essential in composites to guarantee an efficient signal transfer to cells. The conductivity properties were tested by a four-point probe system. PPy is a highly conductive, stable, and biocompatible polymer that has been applied for biosensors, antioxidants, drug delivery, and tissue engineering applications.[44] The conductivity of PPy-containing composites is highly dependent on the synthesis method and the concentration of the conducting polymer.[45] For example, Yang et al. reported that the composition of 1% hyaluronic acid solution with 50 mM of PPy resulted in the conductivity of 7.3 mS cm^{-1},[46] while cellulose/PPy[47] and agarose/PPy[48] composites showed conductivities of 0.08 and 0.1 S cm^{-1}, respectively. In our study, the concentration of 1% PPy did not provide a well-dispersed, homogeneous electrical conductivity along with the films and resulted in partial conductive samples, while increasing the concentration of PPy to 5% facilitated a better chance for conductive chains of polymers to entangle more effectively in the same processing method (Table 1), showing a conductivity of 0.06 S cm^{-1}, which is higher compared with a similar system already reported elsewhere.[31]

Mechanical Properties. The mechanical properties of cardiac patches were tested using the Universal Instron 4240 testing machine, and the mechanical behavior of the conductive composites was compared with that of pure PGS before and after incubation in 1× PBS (pH 7.4) during 21 days. Figure 2a shows the mechanical behavior after incubation in the buffer solution. The cross-linking of ester bonds in the PGS backbone forms a 3D network of random coils of thermoset, which has a rubber-like elastic behavior. This behavior makes PGS an ideal polymer for soft tissues in dynamic mechanical environments, such as the cardiovascular systems.[49] The mechanical properties of PGS are directly associated with the degree of cross-linking and are easily tunable by altering the curing time. The PGS showed an elastic modulus of 0.17 MPa with the curing times of 48 h, which is comparable with other references.[50] The elastic modulus of PGS ranges between 0.05 and 1.5 MPa as reported by Chen et al.[50] PPy is known to change the mechanical properties of composites and hydrogels significantly due to its poor mechanical properties and heterogeneous distribution in the polymer matrix.[51] The presence of PPy in a minor ratio in the

https://dx.doi.org/10.1021/acsami.9b21066
ACS Appl. Mater. Interfaces 2020, 12, 6899−6909

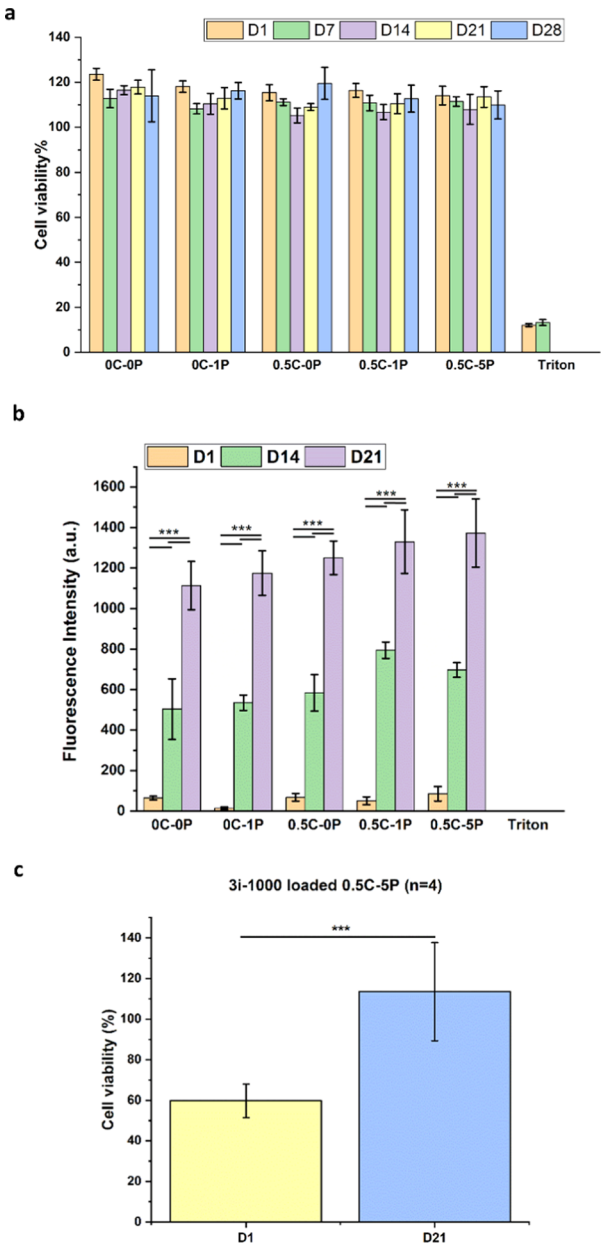

Figure 4. (a) Cytotoxicity of biodegradable patches prepared by the extract method during 28 days in DMEM + 10% FBS. (b) Proliferation of the cardiomyoblast on the surface of the conductive biocomposite during 21 days in DMEM + 10% FBS. (c) Cell viability of 3i-1000 loaded inside the conductive patch compared with the samples without the compound during 21 days.

PGS matrix alters the properties slightly (Table 2). The mechanical properties changed after immersion in 1× PBS, and both types of the samples showed higher elongation (Figure 2a).

Degradation. The degradation speed is a critical factor in the biodegradable composite as it controls the stability of the biomaterials and the drug-releasing process.[52] In our study, the degradation of all types of samples is in the same range, indicating that the addition of 5% PPy does not change the degradation speed of the patch. The composite patches were degraded in a buffer of around 8% for 21 days, which can prevent the drug burst release (Figure 2b). In addition, the degradation and swelling percentage were tested in ethanol and 0.1 M of NaOH and compared with PBS in 24 h of incubation (Figure S3a). The results show that ethanol and NaOH had higher swelling, with the structure swelling more in ethanol compared with that in NaOH; the addition of collagen and PPy up to 5% increased the swelling in NaOH in the same range as in ethanol. Although ethanol swells the structure more, the degradation is less compared with the degradation in NaOH, which is more than 20% (Figure S3b).

Protein Adsorption. Protein adsorption was tested by the BCA protein assay at three different time points of incubation of samples with fetal bovine serum (FBS) to quantify the adsorbed protein on the surface of the patches. Figure 3a shows that the time of incubation did not influence the concentration of the adsorbed proteins, and the saturated amount of the protein is reached at the first time point, at 4 h. However, at 24 h of incubation of the conductive sample in the FBS solution, the protein concentration increases from 35% to more than 40%, when compared with 14 h. In general, the conductive patches show a higher potential to attract proteins, which can be due to the high percentage of hydrophobic PPy.[5]

Drug Release Studies. The release of the small molecule compound 3i-1000 from the bulk of the conductive patch is shown in two different buffers, of MES (pH 6) and PBS (pH 7.4), in Figure 3b. No burst compound release was observed, as the release is based on the degradation of the PGS matrix. PGS degradation can be controlled by changing the sintering parameters, such as curing temperature and time. Here, the temperature and duration of curing was 120 °C in 48 h, which led to the degradation of 8% in 21 days, resulting in the release of more than 20% of the 3i-1000. The compound release increased over time, which is due to the higher degradation percentage of the patch until 80 days. No significant differences were observed in the release of the 3i-1000 in the two different buffers.

The release of adsorbed 3i-1000- and 3i-1000-loaded APTES-TCPSi NPs functionalized on the surface of 0.5C−5P was also studied in MES (pH 6), Figure 3c. The compound physioadsorption efficiency was 12.59 ± 2.08 for the adsorbed 3i-1000, and the encapsulation efficiency (EE %) was 13.47 ± 1.96 for the APTES-TCPSi NP-functionalized patch. The drug release behaviors observed for both systems were similar, showing less than 10% of the cumulative release during 70 days in the MES buffer (pH 6). The results indicate the minor role played by the NPs on loading and the likelihood that 3i-1000 was mainly adsorbed on their surface. Based on Figure 1b, the attached NPs are integrated with the composite matrix and introduce a slightly higher encapsulation efficiency compared with that of the physically adsorbed counterpart, which points to the effect of the surface in the active matrix.

Cell Viability. Cardiomyoblast H9C2 viability was tested during 28 days using the MTT assay to evaluate the cytotoxicity of the cells in a medium containing degraded 2D patches. Figure 4a shows the viable cells and the proliferation in the degraded medium compared with those in the blank incubated medium. This proliferation stays in the same range for 28 days, which shows the biocompatibility of the patch during almost a month. In addition, the AlamarBlue assay shows that the proliferation of the cells increased during 21 days, and the cell number doubled during a week from day 14 until day 21. It can be seen in Figure 4b that the proliferation of the cells on the conductive samples is higher compared with that on the pure PGS samples. In addition, the compound 3i-1000-loaded patches were studied separately and compared

https://dx.doi.org/10.1021/acsami.9b21066
ACS Appl. Mater. Interfaces 2020, 12, 6899−6909

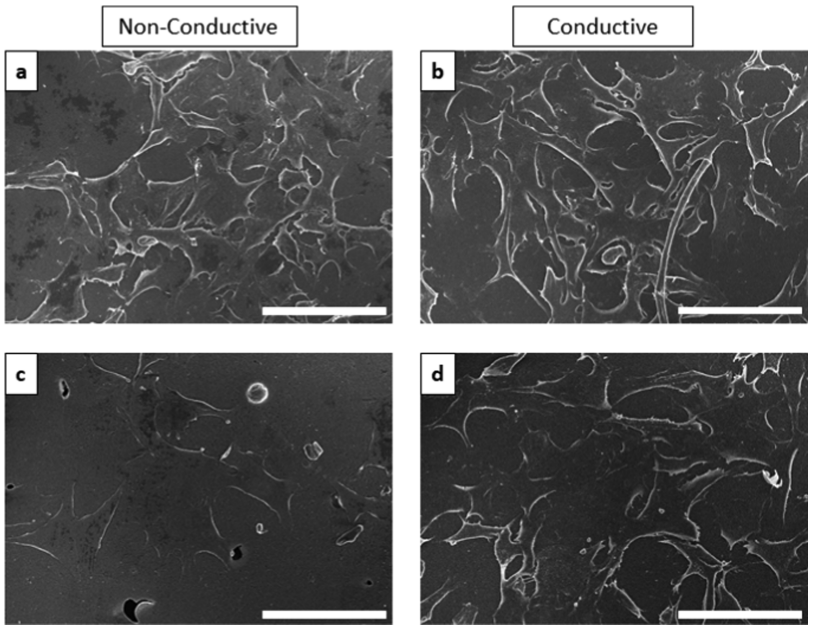

Figure 5. Cardiomyoblast cell attachment on the surface of (a) 0C−0P, (b) 0C−1P, (c) 0.5C−0P, and (d) 0.5C−5P patches on the control and conductive samples during 24 h. Cells were expanded on all samples with high infiltration in the collagen-containing patches. 0.5C−5P attachment shows both high infiltration and attachment within 24 h. Scale bar represents 100 μm.

with the noncompound-loaded samples (Figure 4c). The results show that the 3i-1000 release during 21 days could help the cells to proliferate (AlamarBlue assay) compared with the samples without the compound. Based on the degradation and release experiments, there was ca. 8% of patch degradation and 20% of compound release, which could increase the viability of the cells and increase cell proliferation. Karhu et al.[33] previously showed that the 3i-1000 with a concentration higher than 10 μM showed toxicity in the H9C2 cell line. Although 3i-1000-loaded patches also show toxicity on day 1, 3i-1000 could induce the proliferation for 21 days. This system suggests that the slow release of 3i-1000 from the system is able to provide a safe environment for the cardiomyoblast cells in long-term applications.

Cell Attachment. Early cell attachment was also monitored after 24 h of seeding on the surface of the conductive and nonconductive patches in DMEM−10% FBS. Cells expanded on the surface of all types of samples and showed infiltration (Figure 5). While there was a higher number of cells attached on the conductive samples, higher infiltration was observed in the samples containing collagen. In samples containing collagen and PPy, both great cell attachment and cell infiltration were observed. The conductive patches containing collagen have a high potential to host the cells in the first hours after encountering with the cells, as they can attach and expand on the surface, as well as stay viable based on proliferation results (Figure 4a,b).

CONCLUSIONS

In this study, a drug-loaded conductive biodegradable cardiac patch was developed by the evaporation method. The patch showed excellent cardiomyoblast biocompatibility with high potential for protein and cell attachment in the early hours. The combination of collagen and PPy made a suitable matrix for cells to be attached and infiltrated. Cells were able to proliferate with compound-loaded patches for 21 days compared with the noncompound-loaded patches, demonstrating the ability of this system to deliver the model drug 3i-1000 for cell proliferation. The drug release was based on the degradation of the patch that prevented the burst release. The PPy-based patch showed excellent tensile properties with high elongation, which can even be improved in a wet state suitable for the heart patch implantation condition. The conductive patches show good conductivity, which is important for protein adsorption, wettability, and cell proliferation, compared with the nonconductive samples. Overall, the conductive patches presented here are a smart system for the myocardial infarction applications, based on the combination of PPy, collagen, and PGS with the simultaneous drug-releasing potential.

ASSOCIATED CONTENT

Supporting Information

The Supporting Information is available free of charge at https://pubs.acs.org/doi/10.1021/acsami.9b21066.

Scanning electron microscope image and energy-dispersive X-ray spectroscopy (Figure S1); 0C−0P and 0.5C−5P samples after 5 s and after 48 h immersion in human blood samples (Figure S2); swelling percentage and degradation of composite patches and control samples (Figure S3); and XRD of 3i-1000, and TGA and DSC analysis of 3i-1000 (Figure S4) (PDF)

AUTHOR INFORMATION

Corresponding Author

Hélder A. Santos − *Drug Research Program, Division of Pharmaceutical Chemistry and Technology, Faculty of Pharmacy and Helsinki Institute of Life Science (HiLIFE), University of Helsinki, FI-00014 Helsinki, Finland;* orcid.org/0000-0001-7850-6309; Phone: +358 2941 59661; Email: helder.santos@helsinki.fi

https://dx.doi.org/10.1021/acsami.9b21066
ACS Appl. Mater. Interfaces 2020, 12, 6899−6909

Authors

Nazanin Zanjanizadeh Ezazi − *Drug Research Program, Division of Pharmaceutical Chemistry and Technology, Faculty of Pharmacy, University of Helsinki, FI-00014 Helsinki, Finland*

Rubina Ajdary − *Department of Bioproducts and Biosystems, School of Chemical Engineering, Aalto University, FI-00076 Aalto, Espoo, Finland*

Alexandra Correia − *Drug Research Program, Division of Pharmaceutical Chemistry and Technology, Faculty of Pharmacy, University of Helsinki, FI-00014 Helsinki, Finland*

Ermei Mäkilä − *Laboratory of Industrial Physics, Department of Physics and Astronomy, University of Turku, FI-20014 Turku, Finland;* orcid.org/0000-0002-8300-6533

Jarno Salonen − *Laboratory of Industrial Physics, Department of Physics and Astronomy, University of Turku, FI-20014 Turku, Finland;* orcid.org/0000-0002-5245-742X

Marianna Kemell − *Department of Chemistry, University of Helsinki, FI-00014 Helsinki, Finland;* orcid.org/0000-0002-3583-2064

Jouni Hirvonen − *Drug Research Program, Division of Pharmaceutical Chemistry and Technology, Faculty of Pharmacy, University of Helsinki, FI-00014 Helsinki, Finland*

Orlando J. Rojas − *Department of Bioproducts and Biosystems, School of Chemical Engineering, Aalto University, FI-00076 Aalto, Espoo, Finland; Departments of Chemical & Biological Engineering, Chemistry, and Wood Science, The University of British Columbia, Vancouver, British Columbia V6T 1Z3, Canada;* orcid.org/0000-0003-4036-4020

Heikki J. Ruskoaho − *Drug Research Program, Division of Pharmacology and Pharmacotherapy, University of Helsinki, FI-00014 Helsinki, Finland;* orcid.org/0000-0001-8971-1359

Complete contact information is available at: https://pubs.acs.org/10.1021/acsami.9b21066

Notes

The authors declare no competing financial interest.

■ ACKNOWLEDGMENTS

Prof. H.A.S. acknowledges financial support from the HiLIFE Research Funds, the Sigrid Jusélius Foundation, and the Academy of Finland (decision no. 317042). H.J.R. acknowledges financial support from Business Finland (Finnish Funding Agency for Innovation, Tekes, 3iRegeneration, project 40395/13), the Academy of Finland (project 266661), and the Sigrid Juselius Foundation. Prof. O.J.R. also acknowledges financial support from the H2020-ERC-2017-Advanced Grant "BioELCell" (788489) and the Academy of Finland Centre of Excellence in Molecular Engineering of Biosynthetic Hybrid Materials. The authors thank the Electron Microscopy Unit of the Institute of Biotechnology, University of Helsinki, for providing laboratory facilities and assistance. Dr Flavia Fontana is acknowledged for her kind and generous guidance in this work.

■ REFERENCES

(1) WHO. W.H.O. Cardiovascular Diseases (CVDs). https://www.who.int/en/news-room/fact-sheets/detail/cardiovascular-diseases-(cvds) (accessed May 17, 2017).

(2) Timmis, A.; Townsend, N.; Gale, C.; Grobbee, R.; Maniadakis, N.; Flather, M.; Wilkins, E.; Wright, L.; Vos, R.; Bax, J.; Blum, M.; Pinto, F.; Vardas, P.; Grp, A. W. European Society of Cardiology: Cardiovascular Disease Statistics 2017. *Eur. Heart J.* **2018**, *39*, 508−579.

(3) Haeck, M. L. A.; Hoogslag, G. E.; Rodrigo, S. F.; Atsma, D. E.; Klautz, R. J.; van der Wall, E. E.; Schalij, M. J.; Verwey, H. F. Treatment Options in End-stage Heart Failure: Where to Go Grom Here? *Neth. Heart J.* **2012**, *20*, 167−175.

(4) Tölli, M. A.; Ferreira, M. P. A.; Kinnunen, S. M.; Rysa, J.; Makila, E. M.; Szabo, Z.; Serpi, R. E.; Ohukainen, P. J.; Valimaki, M. J.; Correia, A. M. R.; Salonen, J. J.; Hirvonen, J. T.; Ruskoaho, H. J.; Santos, H. A. In Vivo Biocompatibility of Prous Silicon Biomaterials for Drug Delivery to The Heart. *Biomaterials* **2014**, *35*, 8394−8405.

(5) Ezazi, N. Z.; Shahbazi, M. A.; Shatalin, Y. V.; Nadal, E.; Makila, E.; Salonen, J.; Kemell, M.; Correia, A.; Hirvonen, J.; Santos, H. A. Conductive Vancomycin-Loaded Mesoporous Silica Polypyrrole-Based Scaffolds for Bone Regeneration. *Int. J. Pharm.* **2018**, *536*, 241−250.

(6) Domenech, M.; Polo-Corrales, L.; Ramirez-Vick, J. E.; Freytes, D. O. Tissue Engineering Strategies for Myocardial Regeneration: Acellular Versus Cellular Scaffolds? *Tissue Eng., Part B* **2016**, *22*, 438−458.

(7) Li, X.; Chu, C. L.; Liu, L.; Liu, X. K.; Bai, J.; Guo, C.; Xue, F.; Lin, P. H.; Chu, P. K. Biodegradable Poly-Lactic Acid Based-composite Reinforced Unidirectionally with High-strength Magnesium Alloy Wires. *Biomaterials* **2015**, *49*, 135−144.

(8) Fujimoto, K. L.; Tobita, K.; Guan, J. J.; Hashizume, R.; Takanari, K.; Alfieri, C. M.; Yutzey, K. E.; Wagner, W. R. Placement of an Elastic Biodegradable Cardiac Patch on a Subacute Infarcted Heart Leads to Cellularization With Early Developmental Cardiomyocyte Characteristics. *J. Card. Failure* **2012**, *18*, 585−595.

(9) Fujimoto, K. L.; Tobita, K.; Merryman, W. D.; Guan, J. J.; Momoi, N.; Stolz, D. B.; Sacks, M. S.; Keller, B. B.; Wagner, W. R. An elastic, Biodegradable Cardiac Patch Induces Contractile Smooth Muscle and Improves Cardiac Remodeling and Function in Subacute Myocardial Infarction. *J. Am. Coll. Cardiol.* **2007**, *49*, 2292−2300.

(10) Feiner, R.; Fleischer, S.; Shapira, A.; Kalish, O.; Dvir, T. Multifunctional Degradable Electronic Scaffolds for Cardiac Tissue Engineering. *J. Controlled Release* **2018**, *281*, 189−195.

(11) Qasim, M.; Haq, F.; Kang, M. H.; Kim, J. H. 3D Printing Approaches for Cardiac Tissue Engineering and Role of Immune Modulation in Tissue Regeneration. *Int. J. Nanomed.* **2019**, *14*, 1311−1333.

(12) Ferreira, M. P. A.; Ranjan, S.; Correia, A. M. R.; Makila, E. M.; Kinnunen, S. M.; Zhang, H. B.; Shahbazi, M. A.; Almeida, P. V.; Salonen, J. J.; Ruskoaho, H. J.; Airaksinen, A. J.; Hirvonen, J. T.; Santos, H. A. In Vitro and In Vivo Assessment of Heart-Homing Porous Silicon Nanoparticles. *Biomaterials* **2016**, *94*, 93−104.

(13) Ferreira, M. P. A.; Talman, V.; Torrieri, G.; Liu, D. F.; Marques, G.; Moslova, K.; Liu, Z. H.; Pinto, J. F.; Hirvonen, J.; Ruskoaho, H.; Santos, H. A. Dual-Drug Delivery Using Dextran-Functionalized Nanoparticles Targeting Cardiac Fibroblasts for Cellular Reprogramming. *Adv. Funct. Mater.* **2018**, *28*, No. 1705134.

(14) Kalishwaralal, K.; Jeyabharathi, S.; Sundar, K.; Selvamani, S.; Prasanna, M.; Muthukumaran, A. A Novel Biocompatible Chitosan-Selenium Nanoparticles (SeNPs) Film with Electrical Conductivity for Cardiac Tissue Engineering Application. *Mater. Sci. Eng., C* **2018**, *92*, 151−160.

(15) Tang, J.; Wang, J.; Huang, K.; Ye, Y.; Su, T.; Qiao, L.; Hensley, M. T.; Caranasos, T. G.; Zhang, J.; Gu, Z.; Cheng, K. Cardiac Cell-Integrated Microneedle Patch for Treating Myocardial Infarction. *Sci. Adv.* **2018**, *4*, No. eaat9365.

(16) Feiner, R.; Engel, L.; Fleischer, S.; Malki, M.; Gal, I.; Shapira, A.; Shacham-Diamand, Y.; Dvir, T. Engineered Hybrid Cardiac Patches with Multifunctional Electronics for Online Monitoring and Regulation of TIssue Function. *Nat. Mater.* **2016**, *15*, 679−685.

(17) Loh, X. J.; Karim, A. A.; Owh, C. Poly(Glycerol Sebacate) Biomaterial: Synthesis and Biomedical Applications. *J. Mater. Chem. B* **2015**, *3*, 7641−7652.

(18) Chen, Q. Z.; Ishii, H.; Thouas, G. A.; Lyon, A. R.; Wright, J. S.; Blaker, J. J.; Chrzanowski, W.; Boccaccini, A. R.; Ali, N. N.; Knowles, J. C.; Harding, S. E. An Elastomeric Patch Derived From

Poly(Glycerol Sebacate) for Delivery of Embryonic Stem Cells to The Heart. *Biomaterials* **2010**, *31*, 3885−3893.
(19) Rai, R.; Tallawi, M.; Barbani, N.; Frati, C.; Madeddu, D.; Cavalli, S.; Graiani, G.; Quaini, F.; Roether, J. A.; Schubert, D. W.; Rosellini, E.; Boccaccini, A. R. Biomimetic Poly(Glycerol Sebacate) (PGS) Membranes for Cardiac Patch Application. *Mater. Sci. Eng., C* **2013**, *33*, 3677−3687.
(20) Chen, Q. Z.; Bismarck, A.; Hansen, U.; Junaid, S.; Tran, M. Q.; Harding, S. E.; Ali, N. N.; Boccaccini, A. R. Characterisation of a Soft Elastomer Poly(Glycerol Sebacate) Designed to Match the Mechanical Properties of Myocardial Tissue. *Biomaterials* **2008**, *29*, 47−57.
(21) Jia, Y. T.; Wang, W. Z.; Zhou, X. J.; Nie, W.; Chen, L.; He, C. L. Synthesis and Characterization of Poly(Glycerol Sebacate)-Based Elastomeric Copolyesters for Tissue Engineering Applications. *Polym. Chem.* **2016**, *7*, 2553−2564.
(22) Kharaziha, M.; Nikkhah, M.; Shin, S. R.; Annabi, N.; Masoumi, N.; Gaharwar, A. K.; Camci-Unal, G.; Khademhosseini, A. PGS:Gelatin Nanofibrous Scaffolds with Tunable Mechanical and Structural Properties for Engineering Cardiac Tissues. *Biomaterials* **2013**, *34*, 6355−6366.
(23) Hu, J.; Kai, D.; Ye, H. Y.; Tian, L. L.; Ding, X.; Ramakrishna, S.; Loh, X. J. Electrospinning of Poly(Glycerol Sebacate)-Based Nanofibers for Nerve Tissue Engineering. *Mater. Sci. Eng., C* **2017**, *70*, 1089−1094.
(24) Yang, B.; Lv, W.; Deng, Y. Drug loaded Poly(Glycerol Sebacate) As A Local Drug Delivery System for the Treatment of Periodontal Disease. *RSC Adv.* **2017**, *7*, 37426−37435.
(25) Ravichandran, R.; Venugopal, J. R.; Sundarrajan, S.; Mukherjee, S.; Ramakrishna, S. Cardiogenic Differentiation of Mesenchymal Stem Cells on Elastomeric Poly (Glycerol Sebacate)/Collagen core/Shell fibers. *World J. Cardiol.* **2013**, *5*, 28−41.
(26) Eghbali, M.; Weber, K. T. Collagen and the Myocardium - Fibrillar Structure, Biosynthesis and Degradation in Relation to Hypertrophy and Its Regression. *Mol. Cell. Biochem.* **1990**, *96*, 1−14.
(27) Qazi, T. H.; Rai, R.; Dippold, D.; Roether, J. E.; Schubert, D. W.; Rosellini, E.; Barbani, N.; Boccaccini, A. R. Development and Characterization of Novel Electrically Conductive PANI-PGS Composites for Cardiac Tissue Engineering Applications. *Acta Biomater.* **2014**, *10*, 2434−2445.
(28) Tsui, J. H.; Ostrovsky-Snider, N. A.; Yama, D. M. P.; Donohue, J. D.; Choi, J. S.; Chavanachat, R.; Larson, J. D.; Murphy, A. R.; Kim, D. H. Conductive Silk-Polypyrrole Composite Scaffolds with Bioinspired Nanotopographic Cues for Cardiac Tissue Engineering. *J. Mater. Chem. B* **2018**, *6*, 7185−7196.
(29) Kai, D.; Prabhakaran, M. P.; Jin, G. R.; Ramakrishna, S. Polypyrrole-Contained Electrospun Conductive Nanofibrous Membranes for Cardiac Tissue Engineering. *J. Biomed. Mater. Res., Part A* **2011**, *99A*, 376−385.
(30) Guo, B. L.; Glavas, L.; Albertsson, A. C. Biodegradable and Electrically Conducting Polymers for Biomedical Applications. *Prog. Polym. Sci.* **2013**, *38*, 1263−1286.
(31) Sander, M. M.; Ferreira, C. A. Synthesis and Characterization of a Conductive and Self-Healing Composite. *Synth. Met.* **2018**, *243*, 58−66.
(32) Mäkilä, E.; Bimbo, L. M.; Kaasalainen, M.; Herranz, B.; Airaksinen, A. J.; Heinonen, M.; Kukk, E.; Hirvonen, J.; Santos, H. A.; Salonen, J. Amine Modification of Thermally Carbonized Porous Silicon with Silane Coupling Chemistry. *Langmuir* **2012**, *28*, 14045−14054.
(33) Karhu, S. T.; Valimaki, M. J.; Jumppanen, M.; Kinnunen, S. M.; Pohjolainen, L.; Leigh, R. S.; Auno, S.; Foldes, G.; af Gennas, G. B.; Yli-Kauhaluoma, J.; Ruskoaho, H.; Talman, V. Stem Cells Are the Most Sensitive Screening Tool to Identify Toxicity of GATA4-Targeted Novel Small-Molecule Compounds. *Arch. Toxicol.* **2018**, *92*, 2897−2911.
(34) Kinnunen, S. M.; Tolli, M.; Valimaki, M. J.; Gao, E. H.; Szabo, Z.; Rysa, J.; Ferreira, M. P. A.; Ohukainen, P.; Serpi, R.; Correia, A.; Makila, E.; Salonen, J.; Hirvonen, J.; Santos, H. A.; Ruskoaho, H. Cardiac Actions of a Small Molecule Inhibitor Targeting GATA4-NKX2-5 Interaction. *Sci. Rep.* **2018**, *8*, No. 4611.
(35) Välimäki, M. J.; Tolli, M. A.; Kinnunen, S. M.; Aro, J.; Serpi, R.; Pohjolainen, L.; Talman, V.; Poso, A.; Ruskoaho, H. J. Discovery of Small Molecules Targeting the Synergy of Cardiac Transcription Factors GATA4 and NKX2-5. *J. Med. Chem.* **2017**, *60*, 7781−7798.
(36) Ferreira, M. P. A.; Ranjan, S.; Kinnunen, S.; Correia, A.; Talman, V.; Makila, E.; Barrios-Lopez, B.; Kemell, M.; Balasubramanian, V.; Salonen, J.; Hirvonen, J.; Ruskoaho, H.; Airaksinen, A. J.; Santos, H. A. Drug-Loaded Multifunctional Nanoparticles Targeted to the Endocardial Layer of the Injured Heart Modulate Hypertrophic Signaling. *Small* **2017**, *13*, No. 1701276.
(37) Ravichandran, R.; Venugopal, J. R.; Sundarrajan, S.; Mukherjee, S.; Ramakrishna, S. Poly(Glycerol Sebacate)/Gelatin Core/Shell Fibrous Structure for Regeneration of Myocardial Infarction. *Tissue Eng., Part A* **2011**, *17*, 1363−1373.
(38) Stavrou, B. M.; Beck, C.; Flores, N. A. Changes in Extracellular pH and Myocardial Ischaemia Alter the Cardiac Effects of Diadenosine Tetraphosphate and Pentaphosphate. *Br. J. Pharmacol.* **2001**, *134*, 639−647.
(39) Almeida, P. V.; Shahbazi, M. A.; Makila, E.; Kaasalainen, M.; Salonen, J.; Hirvonen, J.; Santos, H. A. Amine-Modified Hyaluronic Acid-Functionalized Porous Silicon Nanoparticles for Targeting Breast Cancer Tumors. *Nanoscale* **2014**, *6*, 10377−10387.
(40) Yan, Y.; Sencadas, V.; Jin, T. T.; Huang, X. F.; Chen, J.; Wei, D. B.; Jiang, Z. Y. Tailoring the Wettability and Mechanical Properties of Electrospun Poly (L-Lactic Acid)-Poly(Glycerol Sebacate) Core-Shell Membranes for Biomedical Applications. *J. Colloid Interface Sci.* **2017**, *508*, 87−94.
(41) Sajesh, K. M.; Jayakumar, R.; Nair, S. V.; Chennazhi, K. P. Biocompatible Conducting Chitosan/Polypyrrole-Alginate Composite Scaffold for Bone Tissue Engineering. *Int. J. Biol. Macromol.* **2013**, *62*, 465−471.
(42) Yayapour, N.; Nygren, H. Interactions Between Whole Blood and Hydrophilic or Hydrophobic Glass Surfaces: Kinetics of Cell Adhesion. *Colloids Surf., B* **1999**, *15*, 127−138.
(43) Nygren, H. Initial Reactions of Whole Blood with Hydrophilic and Hydrophobic Titanium Surfaces. *Colloids Surf., B* **1996**, *6*, 329−333.
(44) Min, J. H.; Patel, M.; Koh, W. G. Incorporation of Conductive Materials into Hydrogels for Tissue Engineering Applications. *Polymers* **2018**, *10*, 1078.
(45) Thomas, C. A.; Zong, K.; Schottland, P.; Reynolds, J. R. Poly(3,4-Alkylenedioxypyrrole)s As Highly Stable Aqueous-Compatible Conducting Polymers with Biomedical Implications. *Adv. Mater.* **2000**, *12*, 222−225.
(46) Yang, J.; Choe, G.; Yang, S.; Jo, H.; Lee, J. Y. Polypyrrole-Incorporated Conductive Hyaluronic Acid Hydrogels. *Biomater. Res.* **2016**, *20*, 31.
(47) Shi, Z. Q.; Gao, H. C.; Feng, J.; Ding, B. B.; Cao, X. D.; Kuga, S.; Wang, Y. J.; Zhang, L. N.; Cai, J. In Situ Synthesis of Robust Conductive Cellulose/Polypyrrole Composite Aerogels and Their Potential Application in Nerve Regeneration. *Angew. Chem., Int. Ed.* **2014**, *53*, 5380−5384.
(48) Hur, J.; Im, K.; Kim, S. W.; Kim, J.; Chung, D. Y.; Kim, T. H.; Jo, K. H.; Hahn, J. H.; Bao, Z. A.; Hwang, S.; Park, N. Polypyrrole/Agarose-Based Electronically Conductive and Reversibly Restorable Hydrogel. *ACS Nano* **2014**, *8*, 10066−10076.
(49) Wang, Y. D.; Ameer, G. A.; Sheppard, B. J.; Langer, R. A Tough Biodegradable Elastomer. *Nat. Biotechnol.* **2002**, *20*, 602−606.
(50) Chen, Q. Z.; Liang, S. L.; Thouas, G. A. Elastomeric Biomaterials for Tissue Engineering. *Prog. Polym. Sci.* **2013**, *38*, 584−671.
(51) Tomczykowa, M.; Plonska-Brzezinska, M. E. Conducting Polymers, Hydrogels and Their Composites: Preparation, Properties and Bioapplications. *Polymers* **2019**, *11*, 350.
(52) Li, Y.; Chu, Z. W.; Li, X. M.; Ding, X. L.; Guo, M.; Zhao, H. R.; Yao, J.; Wang, L. Z.; Cai, Q.; Fan, Y. The Effect of Mechanical Loads

https://dx.doi.org/10.1021/acsami.9b21066
ACS Appl. Mater. Interfaces 2020, 12, 6899−6909

on the Degradation of Aliphatic Biodegradable Polyesters. *Regener. Biomater.* **2017**, *4*, 179−190.

https://dx.doi.org/10.1021/acsami.9b21066
ACS Appl. Mater. Interfaces 2020, 12, 6899−6909